Dielectric response of surface stabilized ferroelectric liquid crystal cells

Yu. P. Panarin,* Yu. P. Kalmykov,† S. T. Mac Lughadha, H. Xu, and J. K. Vij‡
Department of Microelectronics and Electrical Engineering, University of Dublin, Trinity College, Dublin 2, Ireland
(Received 2 May 1994)

The low-frequency dielectric response of the surface stabilized ferroelectric liquid crystal (SSFLC) cells has been investigated. It was found that the dielectric response depends on the type of the smectic layer structure present and the cell thickness. An analytical solution to the equation of motion that describes the dynamics of SSFLC cells in the presence of a weak external field for both bookshelf and chevron geometries has been developed. This result is used to calculate the dielectric response of these SSFLC cells. Experimental values of the dielectric relaxation strength and the relaxation frequency show good agreement with those predicted by the theoretical model for the chevron structure. An observed discrepancy between the theory and the experimental results for the bookshelf structure is discussed.

PACS number(s): 61.30.Gd, 77.84.Nh, 78.20.Jq, 77.22.Gm

I. INTRODUCTION

Ferroelectric liquid crystals (FLC's) are known to exhibit complex dielectric behavior. In the GHz frequency range there exist two high-frequency modes [1,2]. These are mainly due to the molecular dynamics of the individual molecules. In the frequency range less than 1 MHz, there are two relaxation modes in FLC's corresponding to the collective dynamics of the system [3–6]. The fluctuation in the tilt angle θ gives rise to the soft mode, whereas the fluctuation in the azimuthal angle φ gives rise to the Goldstone mode. The Goldstone mode dielectric response has a lower characteristic frequency and its dielectric relaxation strength is much greater than for the soft mode, except very close to the transition temperature T_c in the smectic-C^* phase (Sm-C^*). By measuring the frequency dependence of the complex dielectric susceptibility, these two contributions can easily be separated from each other [5]. A theory for the dielectric response of a bulk FLC's in the Sm-C^* and Sm-A phase has been carried out by Carlsson *et al.* [6] (see also Ref. [2]). A number of investigators have also studied the dielectric response of FLC's under different conditions (dc bias field, finite sample thickness, etc.) both experimentally and theoretically (see, for example, Refs. [5] and [7–10], and references cited therein). The present paper is concerned with the dielectric study of the low-frequency Goldstone mode in FLC cells in the frequency range 1 Hz to 10 kHz. The Goldstone mode is usually understood to be the fluctuation of the azimuthal angle of the director around the helical axis [3,4]. Recent dielectric measurements [10–14] have shown the existence of at least two relaxation processes in surface stabilized FLC (SSFLC) cells. However, no theoretical description of the Goldstone mode in SSFLC's cells where the helical structure in suppressed by the surface interactions has previously been provided. In this paper, we develop a theoretical model for the dielectric response in both chevron and bookshelf cells and compare the predicted values with those obtained experimentally.

II. THEORY

The dielectric response of the low-frequency Goldstone mode in FLC cells is usually associated with small deformations of the helical structure following the application of an electric field not sufficiently strong so as not to completely unwind the helix [3,4]. The director distribution of the helical structure in the absence of an electric field can be described by the equation $\varphi = qz$, where $q = 2\pi/p_0$ is a wave vector of the helix, p_0 is the helix pitch, φ is the azimuthal angle, and Z is the coordinate axis pointed along the smectic layer normal. The average (macroscopic) polarization (P_S^*) of the helical structure is given by

$$P_S^* = \int_0^{p_0} P_S \cos\varphi(z)\,dz \ , \tag{1}$$

and is equal to zero for the unperturbed helix; P_S is the microscopic spontaneous polarization. Application of an external electric field causes small deformations of the helical structure and gives rise to the macroscopic polarization. The dynamic azimuthal distribution of the spontaneous polarization vector $\mathbf{P}_S$ obeys the equation [5]

$$\gamma_\varphi \sin^2\theta \frac{\partial\varphi}{\partial t} = K_\varphi \sin^2\theta \frac{\partial^2\varphi}{\partial z^2} - P_S E(t)\sin\varphi \ , \tag{2}$$

where γ_φ is the rotational viscosity, K_φ is the elastic constant, and θ is the tilt angle. z is along the Z axis of the helix. The dielectric response for a bulk sample has been investigated both theoretically and experimentally in references by Cava *et al.* [11], Levstik *et al.* [5], and Ostrovskii *et al.* [15]. The solution of Eq. (2) leads to the following expressions for the dielectric strength $\Delta\varepsilon$ and the relaxation time τ_G of the Goldstone mode [5]:

*Permanent address: Organic Intermediates and Dyes Institute, B. Sadovaya, 1/4, Moscow, 103787, Russia.
†Permanent address: Institute of Radio Engineering and Electronics of the Russian Academy of Sciences, Vvedenskii Sq. 1, Fryazino, Moscow Region, 141120, Russia.
‡Author to whom correspondence should be sent.

$$\Delta\varepsilon = \frac{P_S^2}{2\varepsilon_0 K_\varphi (\sin^2\theta) q^2} , \tag{3}$$

$$\tau_G = \frac{\gamma_\varphi}{K_\varphi q^2} , \tag{4}$$

where ε_0 is the permittivity of free space. It is obvious that this description cannot be applied to SSFLC cells where the helix is suppressed by the surface interactions and no director modulation exists along the Z axis. The dielectric properties of such cells have been investigated experimentally [10–13], but no theoretical model has yet been proposed. The dielectric response of SSFLC cells with suppressed helix is found to be independent of the measuring voltage [10–13] in the range of 0–0.2 V and can be fitted to the Havriliak-Negami equation for the frequency dependent complex permittivity [16],

$$\varepsilon^*(\omega) = \varepsilon_\infty + \frac{\Delta\varepsilon}{[1+(i\omega\tau_0)^{(1-\alpha)}]^\beta} , \tag{5}$$

where τ_0 is the most probable relaxation time, ε_∞ is the high-frequency permittivity, and α and β are the parameters that characterize the distribution of the relaxation times. The high-frequency permittivity ε_∞ includes contributions to the total dielectric permittivity from all modes of frequencies higher than the Goldstone mode. The fitting parameters $\alpha \approx 0$ and $\beta \approx 1$ were found for this process, indicating that the relaxation process is described by the Debye equation [Eq. (5) with $\alpha = 0$ and $\beta = 1$] with a single relaxation time. For larger applied voltages (> 0.2 V) another process appears that is strongly nonlinear [13] in nature. This process is due to the different switching mechanisms that occur in FLC's and its classification is beyond the scope of this work, where we are interested only in the linear process occurring at low voltages.

It is well known that in SSFLC cells the director orientation within one type of domain is independent of the Y and Z axes [Figs. 1(a) and 1(b)]; therefore, in order to describe the dynamic distribution of the azimuthal angle of the director under an applied electric field it is reasonable to use the following equation:

$$\gamma_\varphi \sin^2\theta \frac{\partial\varphi}{\partial t} = K_\varphi \sin^2\theta \frac{\partial^2\varphi}{\partial x^2} - P_S E(t) \sin\varphi . \tag{6}$$

This equation describes the dynamic distribution of the azimuthal angle φ with respect to the X axis, which is governed by both the electrostatic interactions and the anchoring at both the substrate surfaces and the chevron interface. Equation (6) differs from Eq. (2) in that the φ is the angle between $\mathbf{P}_s$ and the X axis is the same as that between the director $\mathbf{C}$ and Y axis [Fig. 1(b)]. Henceforth we shall refer to the process described by Eq. (6) as the "X mode" in order to distinguish it from the helical dynamic process described by Eq. (2). This behavior is in contrast to the helical cells where φ is distributed along the Z axis referred to as the "Z mode," which obeys Eq. (2). A similar equation was used by MacLennan *et al.* [17] for the simulation of the electro-optic response in a chevron cell and by Nakagawa [18] for the simulation of the polarization reversed current in a bookshelf cell. We derive an analytical solution of Eq. (6) and use it to describe the dielectric response of both bookshelf and chevron SSFLC cells where, in both cases, the helical structure is suppressed by the surface interactions. The solution of Eq. (6) depends on the boundary conditions, and these conditions are different for the chevron and the bookshelf layer structures. For this reason we shall study these two cases separately.

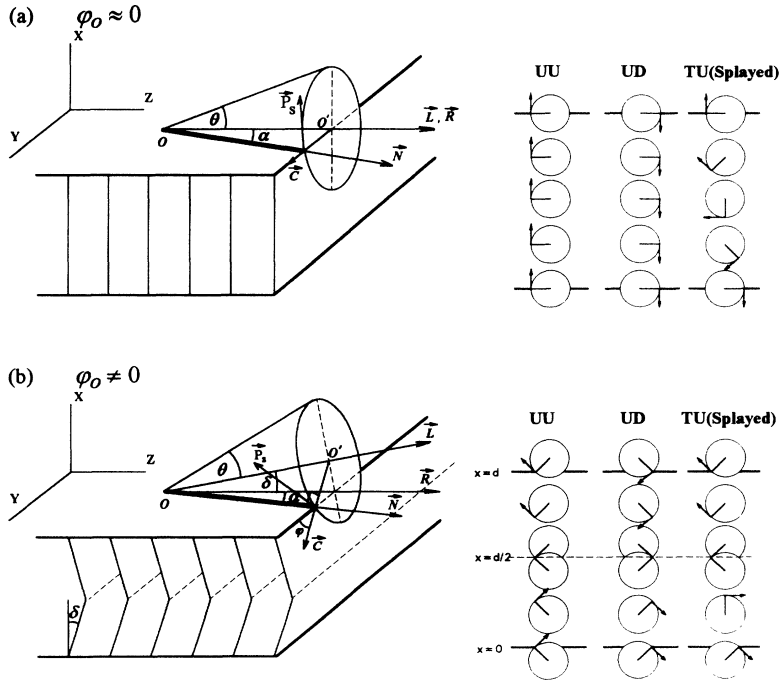

FIG. 1. The smectic layer structure and the coordinate system for FLC cells. (X, Y, Z) is the coordinate system, $\vec{N}$ the molecule director, $\vec{L}$ the smectic layer normal, $\vec{R}$ the rubbing direction, $\vec{C}$ the C director (projection of $\vec{N}$ on smectic layer plane), $\vec{P}_s$ the spontaneous polarization vector, θ the tilt angle, φ the azimuthal angle between the director $\vec{C}$ and the Y axis, φ_0 the azimuthal pretilt angle, α the switching angle (projection of director on electrode), and δ the smectic layer tilt. The abbreviations UU, UD, and TU mean uniform up, uniform down, and twisted up, respectively. (a) Bookshelf; (b) chevron. Figures on the right-hand side have axes: z pointing into the paper, x – vertical and y – horizontal axes.

A. Dielectric response of bookshelf SSFLC cells

The smectic layer structure and the coordinate system for the bookshelf geometry in FLC cells is presented in Fig. 1(a). The only restriction to the dynamics of the director motion is its interactions with the substrate surface. Usually the anchoring energy of FLC with substrates takes into account both polar γ_p, and dispersion γ_d, interactions and can be written in the following form [17,19]:

$$F_s=\pm\gamma_p\cos\varphi-\gamma_d\cos^2(\varphi-\varphi_0)\ , \tag{7}$$

where F_s is the surface density of the anchoring energy, φ_0 is the azimuthal pretilt angle in the absence of an electric field, and the $\pm$ sign indicates that the polar interactions are of opposite sign for the two opposite surfaces. MacLennan *et al.* [17] indicate that φ_0 only affects the dispersion part of the anchoring energy. Boundary conditions are therefore defined by the torque balance at each interface [17,18]; ignoring the polar interaction due to two similar interfaces takes the form

$$K\frac{\partial\varphi}{\partial x}\bigg|_{x=0,d}=\pm\frac{\partial F_s}{\partial\varphi}=\pm\gamma_d\sin2(\varphi|_{x=0,d}-\varphi_0)$$
$$\approx\pm w(\varphi|_{x=0,d}-\varphi_0)\ , \tag{8}$$

where $K=K_\varphi\sin^2\theta$ and $w=2\gamma_d$. Here the $\pm$ signs arise as $\partial\varphi/\partial x$ is positive for $x=0$ and negative for $x=d$. Using the following transformations,

$$\tilde{x}=x/d,\quad \tilde{t}=t/\tau\ ,$$

where

$$\tau=\gamma d^2/K,\quad \gamma=\gamma_\phi\sin^2\theta\ ,$$

Eq. (6) can be written in the dimensionless form as

$$\frac{\partial\varphi}{\partial\tilde{t}}=\frac{\partial^2\varphi}{\partial\tilde{x}^2}-\frac{P_sd^2}{K}E(\tilde{t}\tau)\sin\varphi\ . \tag{9}$$

The normalized boundary conditions from Eq. (8) therefore become

$$\frac{\partial\varphi}{\partial\tilde{x}}\bigg|_{\tilde{x}=0}=\frac{wd}{K}[\varphi(0,t)-\varphi_0]\ , \tag{10}$$

$$\frac{\partial\varphi}{\partial\tilde{x}}\bigg|_{\tilde{x}=1}=-\frac{wd}{K}[\varphi(1,t)-\varphi_0]\ . \tag{11}$$

On applying the linear response theory [20] we first calculate the static dielectric susceptibility, i.e., the dielectric response of the cell subjected to a small constant field E applied along the X axis, and on substituting

$$\varphi(x)=\varphi_0-f(x)+o(E^2)\ ,$$

where $f(x)$ is a term linear in E and $|f(x)|\ll1$, into Eq. (9), we obtain

$$\frac{\partial^2}{\partial\tilde{x}^2}f(\tilde{x})+aE=0\ , \tag{12}$$

where

$$a=\sin\varphi_0P_sd^2/K\ .$$

Equation (12) has a general solution:

$$f(\tilde{x})=-\frac{aE}{2}\tilde{x}^2+C_1\tilde{x}+C_2\ , \tag{13}$$

where the arbitrary constants C_1 and C_2 are to be determined from the boundary conditions Eqs. (10) and (11):

$$C_1=\tfrac{1}{2}aE,\quad C_2=aKE/(2dw)\ .$$

By substituting C_1 and C_2 into Eq. (12) we obtain

$$f(\tilde{x})=-\frac{P_sd^2E}{2K}\left[\tilde{x}^2-\tilde{x}-\frac{K}{wd}\right]\ . \tag{14}$$

Figure 2 shows the static distribution of the azimuthal angle $\varphi(x)$ about its equilibrium position $\varphi=\varphi_0$ for different cell parameters such as the cell thickness, the elastic constant, and the external electric field. It is interesting to note that the deviation of the azimuthal angle from its value in the absence of the field at the surface does not depend on the elastic constant K. The azimuthal angles are given by

$$\varphi(0)=\varphi(1)=\varphi_0-\frac{P_sdE\sin\varphi_0}{2w}\ . \tag{15}$$

The static dielectric susceptibility χ_s is defined as [20]

$$\chi_s=\lim_{E\to0}\frac{P}{E}\ , \tag{16}$$

where P is the projection of P_s onto the direction of the external field, i.e., the X direction, and may be expressed as

$$\chi_s\approx\lim_{E\to0}\frac{P_S}{E}\{[\cos\varphi(0)-\cos\varphi_0]+[\cos\varphi(1)-\cos\varphi_0]\} \tag{17}$$

$$\chi_s=2\lim_{E\to0}\frac{P_S}{E}\left[\cos\left[\varphi_0-\frac{P_sdE\sin\varphi_0}{2w}\right]-\cos\varphi_0\right]\ . \tag{17a}$$

Thus we obtain

$$\chi_s=\frac{P_s^2d\sin^2\varphi_0}{w}\ . \tag{18}$$

We now turn our attention to determining the dynamic response of the cell in the presence of an altering field $E(t)=E\exp(i\omega t)$. Assuming

$$\varphi(\tilde{x},\tilde{t})=\varphi_0-F(\tilde{x})\exp(i\omega\tau\tilde{t})+o(E^2),\quad |F|\ll1\ , \tag{19}$$

and ignoring terms involving powers of E greater than the first, we obtain from Eq. (9)

$$i\omega\tau F(\tilde{x})=\frac{\partial^2F}{\partial\tilde{x}^2}+aE\ . \tag{20}$$

Equation (20) has a general solution,

$$F(\tilde{x})=C_1(\cos\omega_0)\tilde{x}+C_2(\sin\omega_0)\tilde{x}+\frac{aE}{i\omega\tau}\ , \tag{21}$$

where

$$\omega_0^2=-i\omega\tau\ ,$$

and C_1 and C_2 are the arbitrary constants to be determined from the boundary conditions. On substituting

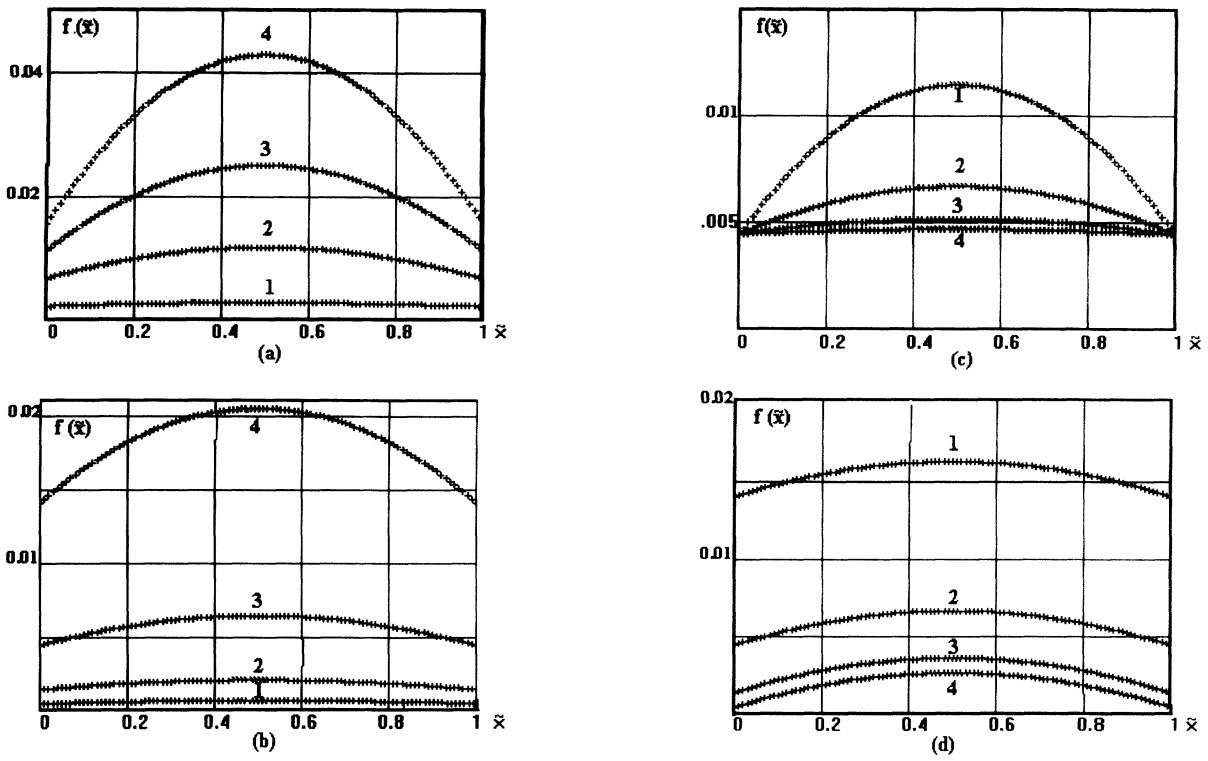

FIG. 2. The static distribution of the azimuthal angle $\varphi(x)$ in degrees about its equilibrium position $\varphi=\varphi_0$ for a cell possessing bookshelf geometry. The basic parameters are $d=10^{-6}$ m, $E=10^2$ V/m, $K=10^{-11}$ J/m^3, $w=10^{-4}$ J/m^2, and $\varphi_0=15°$. For each picture, the curves are numbered 1–4 in order of increasing parameters. (a) Cell thickness (d): 1, 3, 5, and 7 μm; (b) external field (E): 10, 30, 10^2, and 3×10^2 V/m; (c) elastic constant (K): $3\times10^{-11}, 10^{-10}, 3\times10^{-10}$, and 10^{-9} J/m; (d) surface anchoring energy (w): 3×10^{-5}, 10^{-4}, 3×10^{-4}, and 10^{-3} J/m^2.

Eq. (21) into Eqs. (10) and (11), we obtain a set of linear equations for C_1, C_2:

$$C_2\omega_0=\frac{wd}{K}\left[C_1+\frac{aE}{i\omega\tau}\right],$$
$$-\omega_0 C_1\sin\omega_0+C_2\omega_0\cos\omega_0=-\frac{wd}{K}\left[C_1\cos\omega_0+\omega_0\sin\omega_0+\frac{aE}{i\omega\tau}\right],$$

which have the solutions

$$C_1=\frac{aE\,A(\omega)}{i\omega\tau[\omega_0^2K/dw-A(\omega)]},\qquad C_2=\frac{aE}{i\omega\tau[\omega_0^2K/dw-A(\omega)]},\tag{22}$$

where

$$A(\omega)=\frac{(wd/K)\sqrt{-i\omega\tau}\sin\sqrt{-i\omega\tau}-i\omega\tau(1+\cos\sqrt{-i\omega\tau})}{(wd/K)(1-\cos\sqrt{-i\omega\tau})+\sqrt{-i\omega\tau}\sin\sqrt{-i\omega\tau}}.\tag{23}$$

On substituting C_1 and C_2 from Eq. (22) into Eq. (21), we obtain

$$F(\tilde{x})=-\frac{a\,dw\,E}{i\omega\tau[i\omega\tau K+dw\,A(\omega)]}[A(\omega)\cos(\sqrt{-i\omega\tau}\tilde{x})+\sqrt{-i\omega\tau}\sin(\sqrt{-i\omega\tau}\tilde{x})]+\frac{aE}{i\omega\tau}.\tag{24}$$

The complex dielectric susceptibility $\chi(\omega)$ is defined as

$$\chi(\omega)=\lim_{E\to0}\frac{P(t)}{E(t)}.\tag{25}$$

This is found to be [see Eq. (17)]

$$\chi(\omega)=\lim_{E\to0}\frac{P_s}{E\exp(i\omega\tilde{t})}[\cos\varphi(0,\tilde{t}\tau)+\cos\varphi(1,\tilde{t}\tau)-2\cos\varphi_0]=P_s\sin\varphi_0\lim_{E\to0}\frac{1}{E}[F(0)+F(1)],\tag{26}$$

where $F(0)$ and $F(1)$ are the values of $F(\bar{x})$ given by Eq. (24) at $\bar{x}=0$ and $\bar{x}=1$, respectively. On using Eq. (24), Eq. (26) can be rearranged to yield

$$\frac{\chi(\omega)}{\chi_s}=\frac{2}{A(\omega)+i\omega\tau K/dw}\ , \tag{27}$$

where $A(\omega)$ is given by Eq. (23). The dielectric relaxation time τ_D defined as

$$\tau_D=i\lim_{\omega\to 0}\frac{\mathrm{Im}\{\chi(\omega)\}}{\omega\chi_s} \tag{28}$$

can be evaluated from Eq. (23) and (27) by using the Taylor series expansions for trigonometric functions. The result is found to be

$$\tau_D=\frac{\gamma d^2}{12K}\left[1+\frac{6K}{dw}\right]\ . \tag{29}$$

B. Dielectric response of chevron SSFLC cells

Since the discovery by Rieker *et al.* [21], it is now well accepted that on cooling the FLC from the Sm-A to the Sm-C^* phase, the smectic layers no longer remain perpendicular to the substrates but usually possess a tilted chevron structure. This is due to the surface anchoring of the smectic layers in the Sm-A phase, which continue to be anchored during the transition to the Sm-C^* phase. The chevron geometry in SSFLC cells is depicted in Fig. 1(b). We assume that there is no further bending of the smectic layers in the chevron structure when a low external voltage is applied to the cell. From Fig. 1(b) it can be seen that there exist only two possible positions of the director orientation at the chevron interface (i.e., for UU and UD). These two positions will continue to remain fixed so long as low external voltages are applied to the cell. Therefore, in a cell possessing the chevron geometry, the dynamics of the director orientation will be controlled by the anchoring at the substrate surface and the fixed position at the chevron interface.

Using a similar transformation to that given in Sec. II A and putting

$$\bar{x}=\frac{2x}{d},\quad \tilde{t}=\frac{t}{\tau_c}\ ,$$

give

$$\tau_c=\frac{\gamma d^2}{4K}\ . \tag{30}$$

The chevron cell is considered to consist of two identical dielectric slabs separated at the chevron interface; the boundary conditions in dimensionless form become

$$\left.\frac{\partial\varphi}{\partial\bar{x}}\right|_{\bar{x}=0}=\frac{wd}{2K}[\varphi(0,t)-\varphi_0]\ ,$$
$$\varphi(1-0,\tilde{t})=\varphi_0\ ; \tag{31}$$

$$\left.\frac{\partial\varphi}{\partial\bar{x}}\right|_{\bar{x}=2}=-\frac{wd}{2K}[\varphi(2,t)+\varphi_0]\ ,$$
$$\varphi(1+0,\tilde{t})=-\varphi_0\ . \tag{32}$$

On using a mathematical procedure similar to that outlined above and on assuming

$$\varphi(\bar{x})=\begin{cases}\varphi_0-f(\bar{x})+o(E^2) & \text{for } 0\le\bar{x}<1\\ -\varphi_0-f(\bar{x})+o(E^2) & \text{for } 1<\bar{x}\le 2,\end{cases}$$

and using the boundary conditions defined by Eq. (32), we obtain the static solution for the azimuthal angle $\varphi(\bar{x})$:

$$\varphi(\bar{x})=\varphi_0+\frac{P_s d^2E\sin\varphi_0}{8K}\left[\bar{x}^2-\frac{2K+\bar{x}dw}{2K+dw}\right]+o(E^2)$$
$$\text{for } 0\le\bar{x}<1\ ,$$
$$\varphi(\bar{x})=-\varphi_0-\frac{P_s d^2E\sin\varphi_0}{8K}\left[(\bar{x}-2)^2-\frac{2K+(2-\bar{x})dw}{2K+dw}\right]$$
$$+o(E^2)\quad \text{for } 1<\bar{x}\le 2\ . \tag{33}$$

Figure 3 shows $f(\bar{x})$ for different parameters of a chevron cell. These parameters are d, E, K, and w. Let us note that in contrast to the case of the bookshelf cell, where $f(\bar{x})$ was given by Eq. (14), the azimuthal angle at the surfaces for the chevron cells does depend on the elastic constant K.

The static dielectric susceptibility χ_s, can now be obtained from Eq. (16) as

$$\chi_s=\frac{P_s^2d^2\sin^2\varphi_0}{2(2K+dw)}\ . \tag{34}$$

On adopting a similar mathematical procedure to that used in Sec. II A the complex dielectric susceptibility of a SSFLC cell possessing chevron layer structure is found to be

$$\frac{\chi(\omega)}{\chi_s}=\frac{2(dw+2K)}{\sqrt{-i\omega\tau_c}}\frac{(1-\cos\sqrt{-i\omega\tau_c})}{2K\sqrt{-i\omega\tau_c}\cos\sqrt{-i\omega\tau_c}+dw\sin\sqrt{-i\omega\tau_c}}\ . \tag{35}$$

The evaluation of the dielectric relaxation time for the chevron cell τ_D from Eq. (28) leads to the expression

$$\tau_D=\frac{\gamma d^2}{48K}\left[\frac{10K+dw}{2K+dw}\right]\ . \tag{36}$$

Having determined the complex dielectric susceptibility $\chi(\omega)$, we can also calculate the dielectric permittivity $\varepsilon(\omega)$ from the equation

$$\varepsilon(\omega)=\varepsilon_\infty+\frac{\chi(\omega)}{\varepsilon_0}\ .$$

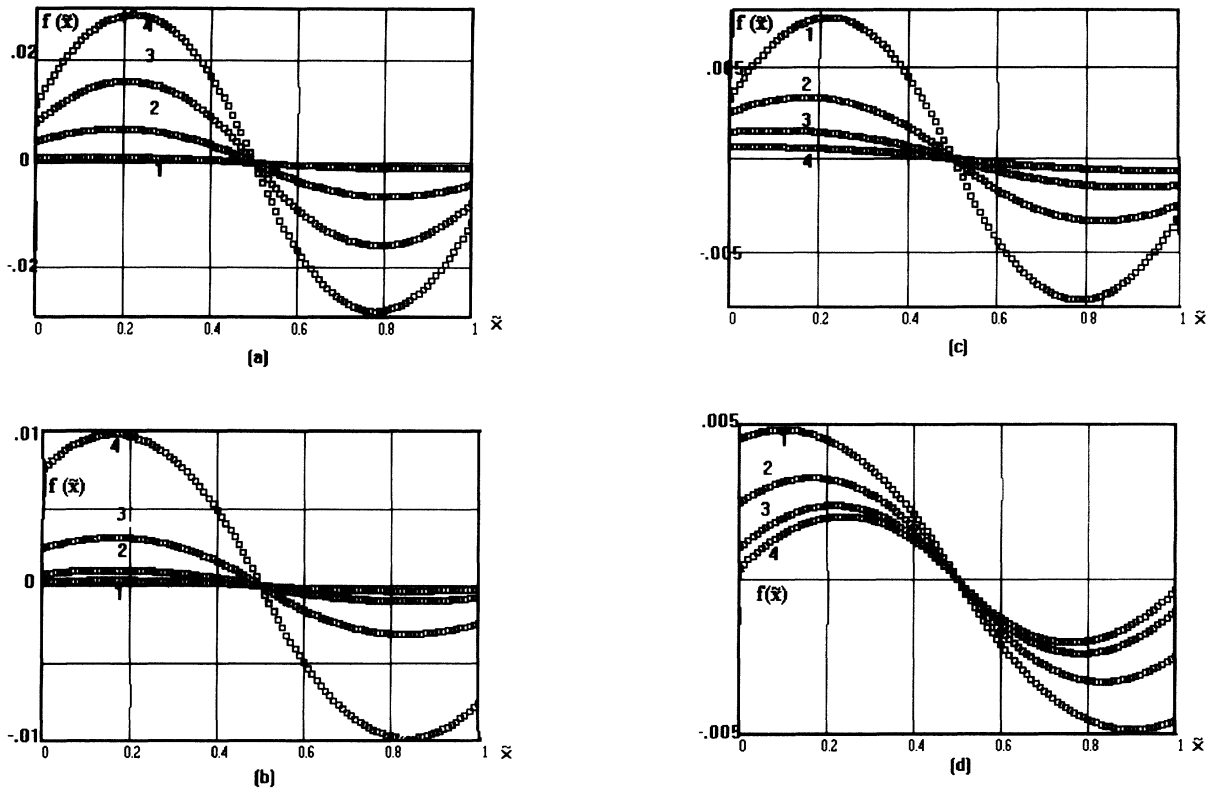

FIG. 3. The static distribution of the azimuthal angle $\varphi(x)$ in degrees about its equilibrium position $\varphi=\varphi_0$ for a cell possessing chevron geometry. The basic parameters are $d=10^{-6}$ m, $E=10^2$ V/m, $K=10^{-11}$ J/m^3, $w=10^{-4}$ J/m^2, and $\varphi_0=60°$. For each picture, the curves are numbered 1–4 in order of increasing parameter. (a) Cell thickness (d): 1, 3, 5, and 7 μm; (b) external field (E): 10, 30, 10^2, and 3×10^2 V/m; (c) elastic constant (K): 3×10^{-11}, 10^{-10}, 3×10^{-10}, 10^{-9} J/m; (d) surface anchoring energy (w): 3×10^{-5}, 10^{-4}, 3×10^{-4}, and 10^{-3} J/m^2.

III. EXPERIMENT

To prepare FLC cells with different smectic layer structures we use FLC mixture SCE 13 (E. Merck) with the following material parameters: $P_s=27$ nC/cm^2, $p_0\approx8$ μm; and the phase sequence

$$\text{Sm-}C^* \xrightarrow[60.8°C]{} \text{Sm-}A \xrightarrow[86.3°C]{} N^* \xrightarrow[100.8°C]{} I ,$$

where N^* denotes chiral nematic and I isotropic phases. Sample cells consisted of indium tin oxide (ITO) coated glass plates. The conducting inner surfaces were spin coated with polyvinyl alcohol (PVA) alignment layer and rubbed parallel. The cells were filled in the isotropic phase of the FLC mixture and then were cooled to the chiral smectic-C (Sm-C^*) phase. To obtain bookshelf structure we apply a high electric field ($E>20$ V/μm) to the SSFLC cells; this results in an irreversible change of the smectic layer structure from the chevron to the striped bookshelf structure. Textures of the experimental cells were observed using a polarizing microscope during the dielectric measurements. Dielectric measurements, in the frequency range 0.1 Hz to 1 MHz were made using a Schlumberger 1255 frequency response analyzer and a Chelsea dielectric interface. This system enabled us to apply direct bias voltage (0–40 V) and alternating voltage (0–3 V_{rms}) simultaneously to the samples during measurements. The dielectric measurements were carried out on the homogeneously aligned (planar) samples; therefore, providing results for $\varepsilon_\perp$ and optical textures could be observed simultaneously using a polarizing microscope.

IV. RESULTS AND DISCUSSION

In order to assess the model described above, we choose the cell thickness as the variable parameter because other parameters used in the model such as K, w, and γ cannot be precisely altered and/or measured. It follows from Eq. (18) that for a cell possessing the *bookshelf* structure there should exist a linear dependence of the static dielectric susceptibility on the thickness of the cell, and accordingly a similar behavior for the dielectric relaxation strength $\Delta\varepsilon$ (defined as twice the maximum of the dielectric loss) should be observed. An approximately quadratic dependence of the relaxation time on the cell thickness should be found. For a cell possessing the chevron structure, Eq. (34) predicts that the dielectric strength should exhibit a linear dependence on the cell thickness for the range $d\gg2K/w$ and a quadratic dependence for the range $d\ll2K/w$; the dependence changes from a quadratic to a linear dependence on increasing the cell thickness. For the chevron cell, Eq. (36) shows that the relaxation time should exhibit an approximately quadratic dependence on the cell thickness.

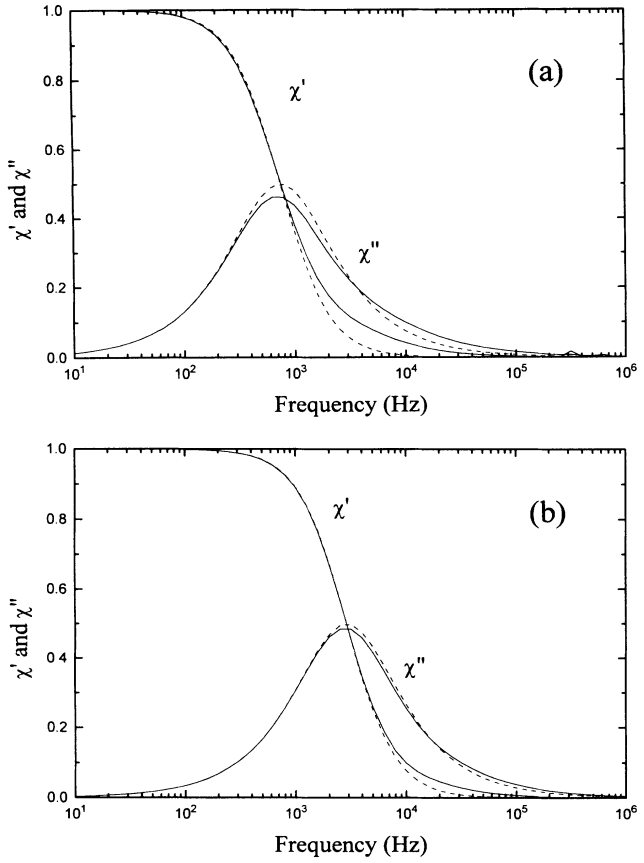

FIG. 4. Calculated normalized frequency dependencies of χ' and χ'' (solid curves) for (a) bookshelf and (b) chevron cells. Dashed curves are the same dependencies predicted by the Debye equation [Eq. (37)] with τ_D from Eqs. (29) and (36). Parameters used are $d=1\times10^{-6}$ m, $K=10^{-11}$ J/m^3, and $w=10^{-4}$ J/m^2, $\gamma=0.1$.

From Eqs. (27) and (35) we are able to calculate the real and imaginary parts of the dielectric susceptibility. Figure 4 shows the frequency dependence of the normalized dielectric susceptibility on frequency for cells possessing bookshelf and chevron structures. The theoretical dependence given by Eqs. (27) and (35) is compared with that predicted by the Debye equation [20]

$$\frac{\chi(\omega)}{\chi_s}=\frac{1}{1+i\omega\tau_D}\ , \tag{37}$$

where the static susceptibility χ_S and the relaxation time τ_D are given by Eqs. (18) and (29) and Eqs. (34) and (36) for the bookshelf and chevron cells, respectively. As seen from Fig. 4 for $\omega\tau_D \leq 1$, the dielectric response of both cells can effectively be described by a simple Debye equation (37).

Figure 5 shows the experimental results for the dependence of the dielectric relaxation strength and the relaxation time on the cell thickness d for chevron cells. As seen from this figure, for cells of thickness $d<20$ μm the dielectric strength $\Delta\varepsilon$ increases linearly with d and the relaxation time increases quadratically as predicted by the theory [Eq. (36)]. This theory cannot be applied to cells of thickness much greater than the pitch of the material. For example, the experimental results show (inset Fig. 5) that for cells of larger thicknesses, $\Delta\varepsilon$ no longer is proportional to d. Furthermore, $\Delta\varepsilon$ and relaxation frequency decrease with increasing thickness until saturation values are reached for cells of thicknesses $d>100$ μm. The dielectric response for such cells is no longer dependent on the cell thickness as determined by the theory of SSFLC cells, but is governed by the helix distortion mode (Z mode). Cells of intermediate thicknesses ($20<d<100$ μm) shall possess a superposition of both the X and Z modes.

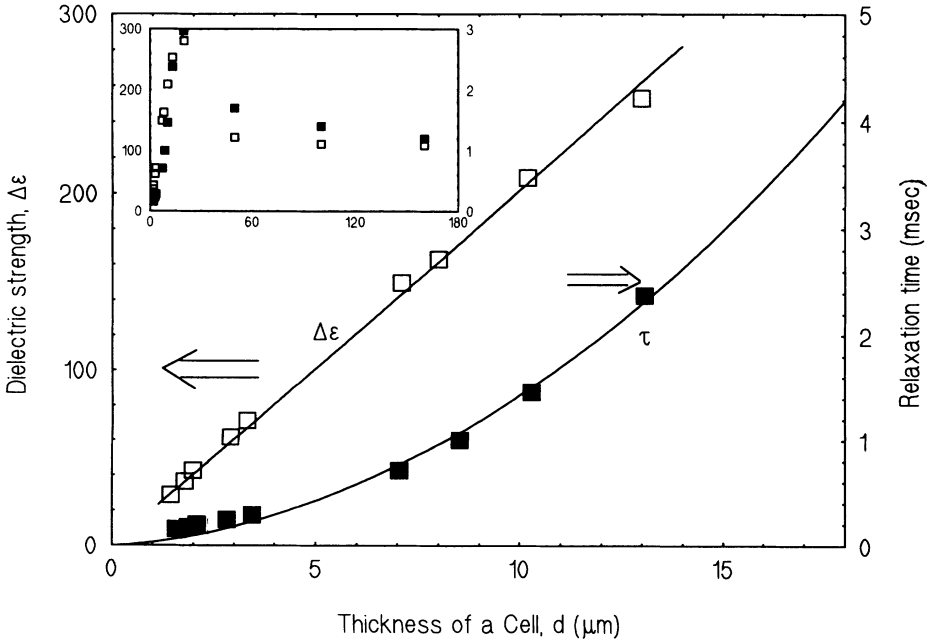

FIG. 5. Experimental results for the dependence of the dielectric relaxation strength (□) and the relaxation time (■) on cell thickness ($d<15$ μm) for chevron cells. The solid curves indicate the best fitted theoretical curves [Eqs. (18) and (29)]. [Inset: Experimental data for cell thickness up to 160 μm (the same symbols and axes apply)].

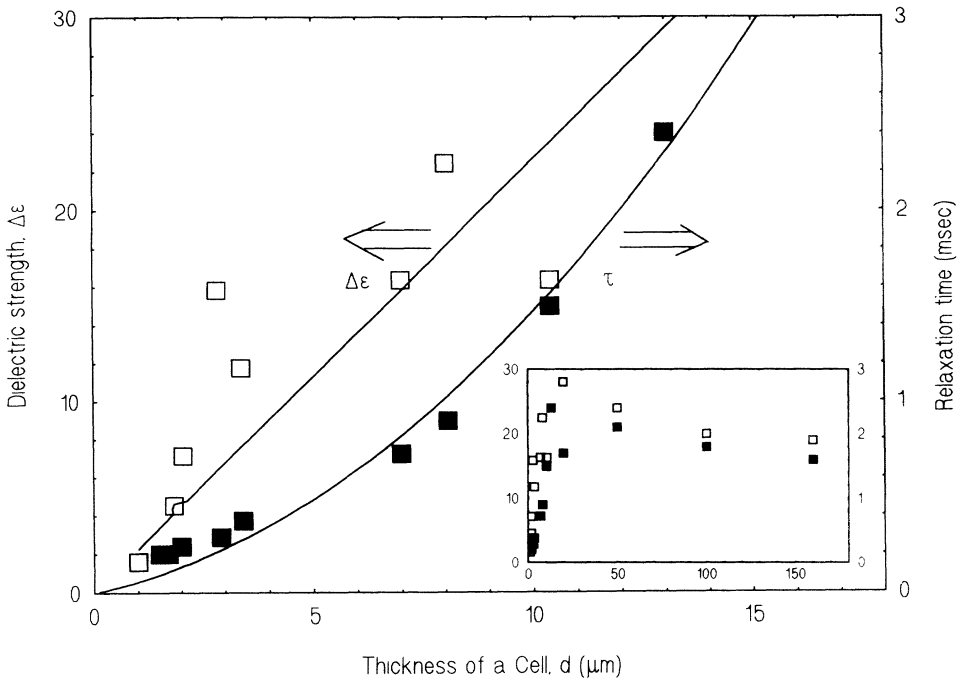

FIG. 6. Experimental results for the dependence of the dielectric relaxation strength (□) and the relaxation time (■) on cell thickness [$(d < 15$ μm)] for bookshelf cells. The solid curves indicate the best fitted theoretical curves [Eqs. (34) and (36)]. [Inset: Experimental data for cell thickness up to 160 μm (the same symbols and axes apply)].

More complicated behavior is observed for cells with the bookshelf structure. For cells possessing such structures, the experimental results for the dependence of the dielectric relaxation strength and the relaxation time on cell thickness d are shown in Fig. 6. As seen from this figure, the relaxation time increases quadratically with the cell thickness (d) and approximately similar values as those for the chevron cells are found. These observations contradict the model presented (Fig. 4) where, according to Eqs. (29) and (36), the relaxation times of the bookshelf and the chevron cells should differ by a factor of

$$\frac{4(dw+6K)(dw+2K)}{dw(dw+10K)} ,$$

which is approximately equal to

$$4 \quad \text{for } K/dw \ll 1$$

and

$$24K/5dw \quad \text{for } K/dw \gg 1 .$$

It may also be seen from Fig. 4 that though $\Delta\varepsilon$ sometimes does vary erratically with d, an overall linear increase of $\Delta\varepsilon$ with d is detected. The explanation for the discrepancies between the experimental results and the theory is given below.

We can reasonably expect that the application of a high electric field to the chevron cell causes an irreversible change of the smectic layer structure from chevron to the bookshelf. According to the model given by Shao, Willis, and Clark [22] the upright positioning of the smectic layers leads to the appearance of two different types of stripes in which the layers normal are turned at an angle $\pm\psi$ to the Z axis. From simple geometrical considerations it can be shown that if the smectic layers become perpendicular to the surface, the angle ψ should be equal to the layer tilt angle δ in the chevron structure. This observed pattern of the electrical field induced striped bookshelf structure nevertheless does not fully explain some of the previous experimental results. Due to the importance of these results on the subject of our study, we consider the discrepancy between the theory and the experimental results in detail.

The essential discrepancy arises from the electro-optical contrast measurements of striped bookshelf FLC cells. The transmittance of the uniform aligned FLC cell between crossed polarizers is expressed as

$$T = \sin^2[2(\beta \pm \theta)]\sin^2\left(\frac{\pi d \Delta n}{\lambda}\right) ,$$

where β is the angle between the polarizer direction and the Z axis of the cell, Δn is the anisotropy in refractive indices, and λ is the wavelength of light. The $\pm$ sign indicates that the angle θ depends on the polarity of the applied voltage. Assuming that the aperture of the light beam is much larger than the width of the individual stripes and $\psi = \delta = k\theta$, then the contrast ratio of the *striped* bookshelf FLC cells between the crossed polarizers can be written in the following form:

$$R = \frac{\sin^2[2(\beta+\theta+k\theta)]+\sin^2[2(\beta+\theta-k\theta)]}{\sin^2[2(\beta-\theta+k\theta)]+\sin^2[2(\beta-\theta-k\theta)]} . \tag{38}$$

In the absence of the striped bookshelf texture (i.e., $k\theta = 0$), the above formula reduces to the general case for the electro-optic contrast ratio. It is found from x-ray investigations [23] that $\delta \approx 0.85\theta$ over a wide range of temperatures. Recent works provided slightly different values of k, but this coefficient is found to lie in the range 0.8–0.9 [21,24]. Figure 7 shows the calculated dependence of the maximum contrast ratio (R) for the striped

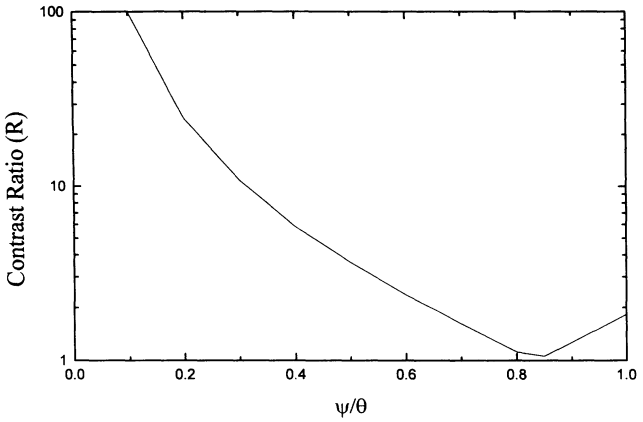

FIG. 7. Calculated dependence of the contrast ratio (R) on ψ/θ for the striped bookshelf cells.

bookshelf cell on the parameter k with a tilt angle $\theta=27°$. The experimental measurements of the angle ψ in the stripes provided by Vorflusev *et al.* [23] showed that the stripes' angle ψ is less than the smectic layer tilt angle in the chevron cell. This results in an experimental value of the contrast ratio to be of the order of 5–10. As can be seen from Fig. 7, the maximum contrast ratio for a reasonable value of $k=0.8-0.9$ is much less than the experimental value [23]. From simple geometry considerations it can be shown that

$$\cos\psi\cos\delta=\cos k\theta \ . \tag{39}$$

This means that the *real* striped "bookshelf" cells in which $\psi<k\theta$ still possess chevron structure but with a smaller value of the layer tilt angle δ. These considerations can also be supported by careful analysis of the experimental results provided by Srajer, Pindak, and Patel [24] from x-ray investigations, which show that the angle of the stripe bookshelf structure $\psi\approx 17-18°$ is slightly less than smectic layer tilt angle in chevron $\delta\approx 20°-21°$.

The somewhat arbitrary behavior of the dielectric strength and the relaxation frequency of the *bookshelf* cells can therefore be explained by the fact that in the striped bookshelf cells the smectic layers are not really perpendicular to the substrate surfaces. Thus to solve the dynamic, Eq. (6), for the bookshelf structure, one should use the boundary conditions for a chevron cell. The experimental values of the relaxation times for the bookshelf cells therefore turn out to be the same as for the chevron cells. The somewhat erratic dependence of the dielectric strength on the cell thickness for the bookshelf cells (Fig. 7) can also be explained by the fact that dielectric strength is strongly dependent on the azimuthal pretilt angle φ_0 [see Eqs. (18) and (34)], which in turn is also dependent on the smectic layer tilt angle through the following relationship:

$$\sin\varphi_0=\tan\delta/\tan\theta \ . \tag{40}$$

Thus the dielectric strength of stripe bookshelf cells should also be strongly dependent on the layer tilt angle which may vary from cell to cell.

V. CONCLUSIONS

A model has been proposed to account for the dielectric properties of SSFLC cells possessing both chevron and bookshelf structures. This model is found to provide good qualitative agreement between theory and experiment for chevron cells with cell thicknesses in the range of 1–20 μm. The thicker cells possess some combination of regions of both uniform and helical orientation of the director, and thus the model is no longer applicable. Bookshelf cells are found to provide relaxation times similar to the chevron ones; however, the theory predicts the relaxation time for the bookshelf cell to be greater than that for a chevron cell by at least a factor of 4. This discrepancy can be explained by taking into account the results of previous electro-optical [23] and x-ray [24] studies. These studies show that striped bookshelf cells do possess a tilted layer structure but with a smaller layer tilt angle than for the case of the chevron structure. Moreover, the "ideal," i.e., orthogonal layer bookshelf structure would seem to be practically unattainable, because even a small deviation of temperature will cause a change in the molecular tilt and consequently a change in the smectic layer tilt. We therefore surmise that it would be of great interest to provide a detailed investigation of the exact smectic layer structure in the so-called *bookshelf* cells so as to clarify these considerations.

ACKNOWLEDGMENTS

We thank Professor B. K. P. Scaife of Dublin and Professor N. A. Clark of Boulder for useful suggestions. This work was partly funded by the EU Grant Nos. SC*0291 and HCM 930353, for which we thank the European Commission.

[1] A. Levstik, T. Carlsson, C. Filipič, I. Levstik, and B. Žekš, Phys. Rev. Lett. **35**, 3527 (1987).
[2] P. G. Costello, Yu. P. Kalmykov, and J. K. Vij, Phys. Rev. A **46**, 4856 (1992).
[3] F. Gouda, K. Skarp, and S. T. Lagerwall, Ferroelectrics **113**, 165 (1991).
[4] J. Pavel, M. Glogarova, and S. S. Bawa, Ferroelectrics **67**, 221 (1987).
[5] A. Levstik, Z. Kutnjak, C. Filipič, I. Levstik, Z. Bregaz, B. Žekš, and T. Carlsson, Phys. Rev. A **42** (4), 2204 (1990).
[6] T. Carlsson, B. Žekš, C. Filipič, and A. Levstik, Phys. Rev. A **42** (2), 877 (1990).
[7] B. Žekš, T. Carlsson, I. Muševič, and B. Kutnjak-Urbanc, Liq. Cryst. **15**, 105 (1993).
[8] Z. Li, R. B. Atkins, G. A. DiLisi, C. Rosenblatt, and R. G. Petschek, Phys. Rev. A **43**, 852 (1991).
[9] Yu. P. Kalmykov, J. K. Vij, H. Xu, A. Rappaport, and M. D. Wand, Phys. Rev. E **50**, 2109 (1994).

[10] F. M. Gouda, Ph.D. thesis, Chalmers University of Technology, Göteborg, Sweden, 1992.
[11] R. J. Cava, J. S. Patel, K. R. Collen, J. W. Goodby, and E. A. Rietman, Phys. Rev. A **35**, 4378 (1987).
[12] J. Zubia, A. Ezcurra, M. R. De La Fuenta, and M. A. Perez Jubindo, Liq. Cryst. **10**, 849 (1991).
[13] Yu. P. Panarin, H. Xu, S. T. Mac Lughadha, and J. K. Vij, Jpn. J. Appl. Phys. **33**, 2648 (1994).
[14] M. Marzec, W. Haase, E. Jakob, M. Pfeiffer, S. Wróbel, and T. Geelhaar, Liq. Cryst. **14**, 1967 (1993).
[15] B. I. Ostrovskii, A. Z. Rabinovich, A. S. Sonin, and B. A. Strukov, Zh. Eskp. Teor. Fiz. **74**, 1748 (1978) [Sov. Phys. JETP **47**, 912 (1978)].
[16] S. Havriliak and S. Negami, J. Polym. Sci. **C14**, 99 (1966).
[17] J. E. MacLennan, M. A. Handschy, and N. A. Clark, Liq. Cryst. **7**, 787 (1990); J. E. MacLennan, N. A. Clark, M. A. Handschy, and M. R. Meadows, *ibid.* **7**, 753 (1990).
[18] M. Nakagawa, Mol. Cryst. Liq. Cryst. **173**, 1 (1989).
[19] M. A. Handschy, N. A. Clark, and S. T. Lagerwall, Phys. Rev. Lett. **51**, 47 (1983).
[20] B. K. P. Scaife, *Principles of Dielectrics* (Clarendon, Oxford, 1989).
[21] T. P. Rieker, N. A. Clark, G. S. Smith, D. S. Parmar, E. B. Sirota, and C. R. Safinya, Phys. Rev. Lett. **59**, 2658 (1987).
[22] R. F. Shao, P. C. Willis, and N. A. Clark, Ferroelectrics **121**, 127 (1991).
[23] V. P. Vorflusev, Yu. P. Panarin, S. A. Pikin, and V. G. Chigrinov, Liq. Cryst. **14**, 1055 (1993).
[24] S. Srajer, R. Pindak, and J. S. Patel, Phys. Rev. A **43**(10), 5744 (1990).